

UCLA

UCLA Previously Published Works

Title

Enantioselective Synthesis of Quaternary Oxindoles: Desymmetrizing Staudinger–Aza–Wittig Reaction Enabled by a Bespoke HypPhos Oxide Catalyst.

Permalink

<https://escholarship.org/uc/item/12r615df>

Journal

Journal of the American Chemical Society, 144(46)

Authors

Xie, Changmin

Kim, Jacob

Mai, Binh

et al.

Publication Date

2022-11-23

DOI

10.1021/jacs.2c09421

Peer reviewed



Published in final edited form as:

*J Am Chem Soc.* 2022 November 23; 144(46): 21318–21327. doi:10.1021/jacs.2c09421.

## Enantioselective Synthesis of Quaternary Oxindoles: Desymmetrizing Staudinger–Aza-Wittig Reaction Enabled by a Bespoke HypPhos Oxide Catalyst

**Changmin Xie,**

Department of Chemistry and Biochemistry, University of California Los Angeles, Los Angeles, California 90095-1569, United States

**Jacob Kim,**

Department of Chemistry and Biochemistry, University of California Los Angeles, Los Angeles, California 90095-1569, United States

**Binh Khanh Mai,**

Department of Chemistry and Biochemistry, University of California Los Angeles, Los Angeles, California 90095-1569, United States

**Shixuan Cao,**

Department of Chemistry and Biochemistry, University of California Los Angeles, Los Angeles, California 90095-1569, United States

**Rong Ye,**

Department of Chemistry and Biochemistry, University of California Los Angeles, Los Angeles, California 90095-1569, United States

**Xin-Yi Wang,**

Department of Chemistry and Biochemistry, University of California Los Angeles, Los Angeles, California 90095-1569, United States

**Peng Liu,**

Department of Chemistry, University of Pittsburgh, Pittsburgh, Pennsylvania 15260, United States

**Ohyun Kwon**

---

**Corresponding Authors:** **Peng Liu** – Department of Chemistry, University of Pittsburgh, Pittsburgh, Pennsylvania 15260, United States; pengliu@pitt.edu, **Ohyun Kwon** – Department of Chemistry and Biochemistry, University of California Los Angeles, Los Angeles, California 90095-1569, United States; ohyun@chem.ucla.edu.

The authors declare no competing financial interest.

### ASSOCIATED CONTENT

#### Supporting Information

The Supporting Information is available free of charge at <https://pubs.acs.org/doi/10.1021/jacs.2c09421>.

Full experimental procedures and analytical data ( $^1\text{H}$ ,  $^{13}\text{C}$ ,  $^{19}\text{F}$ , and  $^{31}\text{P}$  NMR spectral data; HPLC, HRMS, and X-ray crystallographic data) for new compounds (PDF)

#### Accession Codes

CCDC 2205082 contains the supplementary crystallographic data for this paper. These data can be obtained free of charge via [www.ccdc.cam.ac.uk/data\\_request/cif](http://www.ccdc.cam.ac.uk/data_request/cif), or by emailing [data\\_request@ccdc.cam.ac.uk](mailto:data_request@ccdc.cam.ac.uk), or by contacting The Cambridge Crystallographic Data Centre, 12 Union Road, Cambridge CB2 1EZ, UK; fax: +44 1223 336033.

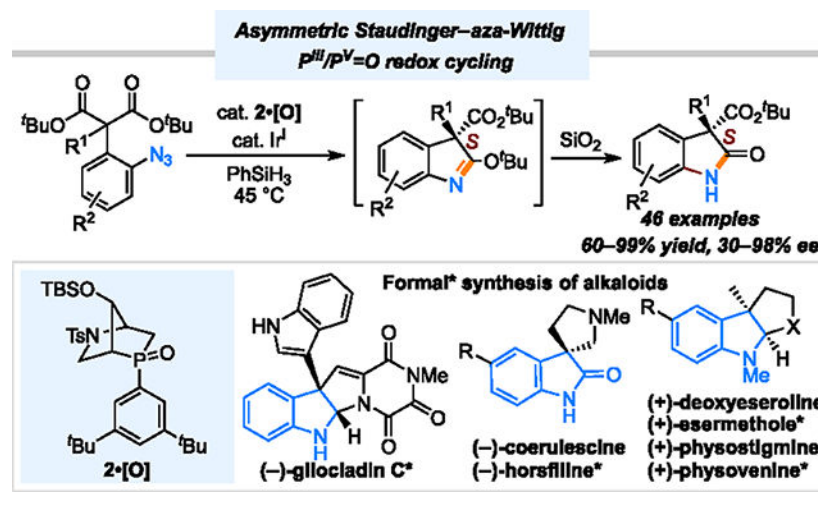
Complete contact information is available at: <https://pubs.acs.org/10.1021/jacs.2c09421>

Department of Chemistry and Biochemistry, University of California Los Angeles, Los Angeles, California 90095-1569, United States

## Abstract

This paper describes a catalytic asymmetric Staudinger–aza-Wittig reaction of (*o*-azidoaryl)malonates, allowing access to chiral quaternary oxindoles through phosphine oxide catalysis. We designed a novel HypPhos oxide catalyst to enable the desymmetrizing Staudinger–aza-Wittig reaction through the  $P^{III}/P^V=O$  redox cycle in the presence of a silane reductant and an  $Ir^I$ -based Lewis acid. The reaction occurs under mild conditions, with good functional group tolerance, a wide substrate scope, and excellent enantioselectivity. Density functional theory revealed that the enantioselectivity in the desymmetrizing reaction arose from the cooperative effects of the  $Ir^I$  species and the HypPhos catalyst. The utility of this methodology is demonstrated by the (formal) syntheses of seven alkaloid targets: (–)-gliocladin C, (–)-coerulescine, (–)-horsfilline, (+)-deoxyeseroline, (+)-esermethole, (+)-physostigmine, and (+)-physovenine.

## Graphical Abstract



## INTRODUCTION

Organic phosphorus compounds are powerful reagents for the construction of  $C=C$  and  $C=N$  bonds through Wittig and aza-Wittig reactions.<sup>1,2</sup> Although many catalytic versions of these reactions have been reported to avoid the formation of phosphine oxide waste through  $P^{III}/P^V=O$  redox cycling mediated by silanes,<sup>3,4</sup> catalytic enantioselective versions of Wittig and aza-Wittig reactions involving  $P^{III}/P^V=O$  redox cycling are rare.<sup>5</sup> Werner et al. reported the first catalytic asymmetric Wittig reaction through desymmetrization of cyclopentane-1,3-dione with Me-DuPhos as the catalyst and phenylsilane as the terminal reductant.<sup>6</sup> The Christmann group reinvestigated Werner's asymmetric transformation and applied it in the total syntheses of *ent*-dichrocephone A and *ent*-dichrocephone B.<sup>7</sup> The Voituriez group developed an asymmetric  $\alpha$ -umpolung addition–Wittig olefination cascade to access chiral (trifluoromethyl)cyclobutenes using *exo*-anisyl-HypPhos oxide as the catalyst and phenylsilane as the reductant.<sup>8</sup> The Staudinger–aza-Wittig reaction figures

prominently in the formation of nitrogen-containing compounds, especially heterocycles.<sup>2</sup> Despite the usefulness of the Staudinger–aza-Wittig reaction, asymmetric Staudinger processes are even rarer than asymmetric Wittig reactions.<sup>5</sup> In early examples, kinetic resolution of racemic azides (Figure 1A)<sup>9</sup> and desymmetrization of a 1,3-diketone (Figure 1B)<sup>10</sup> were realized by applying stoichiometric amounts of phosphines. Although Werner had achieved high enantioselectivity with P<sup>III</sup>/P<sup>V</sup>=O redox cycling at high temperature (150 °C),<sup>6,7</sup> it would be preferable to have milder conditions for phosphine oxide recycling in asymmetric transformations. We and others have demonstrated that strained phosphines facilitate P<sup>III</sup>/P<sup>V</sup>=O redox cycling mediated by hydrosilanes under mild conditions.<sup>11,12</sup> Accordingly, in a previous study, we developed a catalytic asymmetric Staudinger–aza-Wittig reaction of 1,3-diones, using our chiral phosphine HypPhos **1**, for the synthesis of heterocyclic amines (Figure 1C).<sup>13</sup> In recognition of the importance of the Staudinger–aza-Wittig reaction for synthesizing heterocycles, we wondered whether chiral lactams could be accessed through a Staudinger–aza-Wittig reaction and applied to the syntheses of complex alkaloids.

Oxindoles and indolines bearing a C3-quaternary stereocenter are core structures of a diverse range of natural products and pharmaceuticals (Figure 1D).<sup>14,15</sup> As such, many enantioselective processes have been developed to access chiral quaternary oxindoles,<sup>15</sup> with most relying on stereoselective functionalization of pendant alkenes (e.g., through Heck-type reactions,<sup>16a–f</sup> cyanoamidation,<sup>16g</sup> or Ni-catalyzed dicarbofunctionalization<sup>16h,i</sup>) or existing oxindoles (e.g., through alkylation,<sup>17a,b</sup> Michael addition,<sup>17c</sup> Claisen rearrangement,<sup>17d</sup> Mannich,<sup>17e</sup> aldol,<sup>17f</sup> allylation,<sup>17g</sup> or acyl-migration<sup>17h,i</sup> approaches). Departing from those previous routes, we turned to a desymmetrization strategy (Figure 1D).<sup>18,19</sup> We envisioned that the chiral iminophosphorane intermediate formed from a prochiral 2-(*o*-azidoaryl)malonate **3** would differentiate its two ester units with enantioselective formation of an imidate through an aza-Wittig reaction. The resulting imidate would readily hydrolyze to give a lactam **4** with the quaternary stereogenic center unchanged. Previously reported Staudinger–aza-Wittig reactions of esters have been performed under harsh conditions (e.g., reflux in toluene).<sup>2,20,21</sup> In terms of the relatively low reactivity of esters and the challenges of asymmetric induction, we surmised that coordination of a Lewis acid and a chiral iminophosphorane might facilitate the aza-Wittig reaction of unactivated esters, considering that both 1,3-dicarbonyl groups and iminophosphoranes are good ligands for Lewis acids.<sup>22,23</sup> Moreover, Lewis acids can facilitate silane-mediated reductions of phosphine oxides, potentially assisting the P<sup>III</sup>/P<sup>V</sup>=O redox cycling in this present case.<sup>4,24</sup> Accordingly, we applied a custom-made HypPhos oxide catalyst, **2**•[O], to the synthesis of valuable quaternary oxindoles, with the aid of cooperative Ir<sup>I</sup>–P<sup>III</sup>/P<sup>V</sup>=O redox cycling.

## RESULTS AND DISCUSSION

Initially, we tested the commercially available [2.2.1] bicyclic chiral phosphines (“HypPhos” derivatives) **1** and **5**<sup>25</sup> for their suitability in the Staudinger–aza-Wittig reaction of the malonate **3a** (Table 1). A stoichiometric amount of *endo*-phenyl-HypPhos **1** provided efficiency and enantioselectivity (58% ee) better than those of *exo*-phenyl-HypPhos **5** (11% ee) (entries 1 vs 2). An attempt to lower the reaction temperature (from 70 to 40 °C) to increase the enantioselectivity produced only a trace amount of product (entry 3).

Hypothesizing that a Lewis acid might enhance the electrophilicity of the malonate ester<sup>22,23</sup> and promote the silane-mediated reduction of the phosphine oxide,<sup>4,24</sup> we surveyed a variety of metal salts for the reactions involving the HypPhos oxide **1•[O]** (air-stable and, therefore, easier to handle than its tertiary phosphine counterpart) and phenylsilane.<sup>26</sup> Because both the phosphine ligand and metal ion were present in the reaction, we were cognizant that “self-quenching” might possibly preclude the Staudinger–aza-Wittig reaction.<sup>27</sup> To our delight, adding both CuF<sub>2</sub> and PhSiH<sub>3</sub> allowed the reaction to proceed at a lower temperature (35 °C) and produced **4a** with improved enantioselectivity (78% ee) (entry 4). In the absence of molecular sieves, the ee of the product varied, presumably because of racemization arising from hydrolysis of the imidate product. Switching the solvent from toluene to less polar cyclohexane slightly improved the enantioselectivity (82% ee), although the conversion was lower and the isolated yield was only 50% (entry 5). We reasoned that the low conversion might have resulted from self-quenching between the metal and phosphine. To alleviate that deleterious effect, we designed a series of “bulkier” phosphines that would presumably dissociate more readily from the transition metal ion. The most straightforward approach was the incorporation of a bulky aryl substituent on the phosphorus atom. Again to our delight, the use of *endo*-(3,5-di-*tert*-butylphenyl)-HypPhos oxide (**6•[O]**) under otherwise identical conditions produced the oxindole **4a** in a good isolated yield, albeit with slightly decreased stereoselectivity (92%, 77% ee) (entry 6).

In an attempt to increase the enantioselectivity, we modified the [2.2.1]-bicyclic skeleton of the catalyst, obtaining the *endo*-phenyl-7-trimethylsiloxy-HypPhos oxide **7•[O]** from commercially available L-proline.<sup>26</sup> Employing the HypPhos oxide **7•[O]** improved the enantioselectivity (89% ee) but decreased the reaction efficiency (30% isolated yield, entry 7). Thus, we combined a 3,5-di-*tert*-butylphenyl substituent on the phosphorus center and a trimethylsiloxy group at the apical carbon atom to assemble the phosphine oxide **8•[O]**, which admirably catalyzed the conversion of the malonate **3a** to the oxindole **4a** in excellent yield and with good enantioselectivity (95%, 87% ee, entry 8). Changing the Lewis acid from CuF<sub>2</sub> to [Ir(*cod*)Cl]<sub>2</sub> further improved the enantioselectivity (95%, 92% ee, entry 9). Here, we added tetrabutylammonium tetrafluoroborate (TBABF<sub>4</sub>), along with [Ir(*cod*)Cl]<sub>2</sub>, to facilitate its chloride ion exchange.<sup>28</sup> In the absence of TBABF<sub>4</sub>, the reaction was very slow (see Table S6 for details). When we performed the reaction at 45 °C, we could decrease the loadings of **8•[O]** and [Ir(*cod*)Cl]<sub>2</sub> to 10 and 5 mol %, respectively, while maintaining the yield and enantioselectivity (95%, 93% ee, entry 10). A survey of various silyl groups indicated that the TBS unit was optimal (entries 10–13). The yield and selectivity were comparable when employing 3 or 4 equiv of PhSiH<sub>3</sub> (cf. entries 14 and 12), but further decreasing it to 2 equiv diminished the yield (entry 15).

On examining the scope of the transformation, we found that malonates substituted with simple alkyl substituents (**3a–e**) gave their oxindoles (**4a–e**) in good yields (87–98%) and excellent enantioselectivities (92–94% ee), except in the case of the malonate with a methyl substituent (**3b**), where the selectivity was lower (68% ee) (Table 2A). A substrate having an acid-sensitive dimethyl acetal functional group (**3f**) was tolerated, with the corresponding oxindole **4f** isolated in 88% yield and 91% ee. Substrates with silyl ether substituents (**3g–i**) also reacted well to form their oxindoles (**4g–i**) in good yields (97–99%) and with moderate

selectivity (85–87% ee). The malonate **3f** substituted with a (5-triisopropylsiloxy)pentyl group displayed improved enantioselectivity (91% ee) but lower yield (80%). Interestingly, the oxindole with a (3-ethoxycarbonyl)propyl substituent (**4k**) was obtained with lower selectivity (83% ee), presumably because of coordination of the ethyl ester unit to the Lewis acid, diminishing the effects of the latter in promoting the reactivity and enantioselectivity (vide infra). Malonates possessing sterically bulkier *tert*-butyl ester (**3l**) and more-electron-deficient phenyl ester (**3m**) units, which coordinate poorly when compared with ethyl ester units, behaved better, forming their oxindoles (**4l–m**) with improved yields (86–91%) and enantioselectivities (89–91% ee). Malonates substituted with  $\alpha$ -benzyl groups were also suitable substrates (**3n–u**). For example, we isolated oxindoles with benzyl and fluoro- and pinacol boronic ester (Bpin)-substituted benzyl groups (**4n–p**) in good yields (68–99%) and excellent selectivity (90–93% ee). The specific rotation of our product (+)-**4n** was opposite to that of the known oxindole (*R*)-**4n**,<sup>29</sup> allowing us to assign the *S* configuration to our oxindole product. In other examples, we isolated oxindoles with protected indole units (**4q** and **4r**) and an aza-indole (**4t**) in high yields (88–98%) and good selectivity (88–91% ee). The substrate with an unprotected indole moiety (**3s**) produced its oxindole **4s** in good yield (96%), but the enantioselectivity was lower (86% ee). When we subjected the substrate **3u** (containing a pyridine heterocycle) to the reaction conditions, we observed the formation of the relatively stable imidate **11u**, which could be purified through NEt<sub>3</sub>neutralized silica gel column chromatography in good yield (90%) and selectivity (91% ee). The isolation of this imidate indicated that the mechanism of our Staudinger–aza-Wittig reaction, between an azide and an ester, differed from those of Staudinger ligations used previously in chemical biology.<sup>30</sup> For the malonates with 3-phenylpropyl (**3v**) and 3-(naphth-2-yl)propyl (**3w**) substituents, we isolated their oxindoles in good yields (75–80%) and excellent enantioselectivities (92–93% ee). We obtained the heteroatom-substituted oxindole **4x** in excellent yield (99%) but with lower selectivity (30% ee).

Subsequently, we investigated malonates substituted with various *o*-azidoaryl groups (Table 2B). Oxindoles bearing electron-donating groups at the C6 position (**4y–aa**) were produced in good yields (97–99%) and excellent enantioselectivities (90–93% ee). An aromatic substituent at the C6 position could be tolerated, with the oxindole **4ab** obtained in 99% yield and 90% ee. Other electron-withdrawing groups at the C6 position were also compatible (**3ac–ae**), with the corresponding oxindoles **4ac–ae** isolated in good yields (83–97%) and enantioselectivities (89–94% ee). Substrates bearing halides at the C6 position (**3af–ah**) reacted well to give their oxindoles (**4af–ah**) in good yields (80–88%) and excellent enantioselectivities (91–95% ee). The enantioselectivity for the reaction of the 5-MeO oxindole was lower (**4ai**, 81% ee), but changing the MeO group to a less electron-donating tosyl group (**4aj**) increased the selectivity to 91% ee. Trifluoromethyl and fluoro groups at the C5 position (**4ak–am**) were tolerated, with the corresponding oxindoles isolated in good yields (91–95%) and enantioselectivities (87–93% ee). We prepared the C7-substituted oxindole **4an** in commendable yield (98%) and enantioselectivity (96% ee). When multiple halide atoms were present on the aromatic rings (**3ao** and **3ap**), the Staudinger–aza-Wittig reactions proceeded smoothly to give the desired products (**4ao** and **4ap**) in excellent yields (91–94%) and enantioselectivities (93% ee). Azido substrates featuring pyridine and quinoline units reacted to furnish the aza-oxindole **4aq**,



the aza-imidate **11ar**, and the fused aza-oxindole **4as** in high yields (92–94%) and enantioselectivities (94–98% ee). Because the electron-deficiency of these heterocycles decreased the reactivity of the resulting iminophosphoranes, with the basic nitrogen atoms possibly coordinating to the Lewis acid, higher catalyst loadings {**2•[O]** (25 mol %), [Ir(*cod*)Cl]<sub>2</sub> (12.5 mol %)} and a longer reaction time (72 h) were required to ensure high conversions. Interestingly, the imidate **11ar** could also be purified, through column chromatography using NEt<sub>3</sub>-neutralized silica gel, in 92% isolated yield. A bidirectional Staudinger–aza-Wittig reaction afforded the oxindole **4at** in 85% yield, with 5.3:1 dr and 90% ee. Notably, cyclization of the amine to the oxindole **4at** without the catalyst resulted in a 1:1.7 dr, favoring the formation of the meso-oxindole.

To demonstrate the synthetic utility of this methodology, we first performed the reaction of **3f** on a 2.1 g scale (Scheme 1A). Using a lower catalyst loading {**2•[O]** (5 mol %), [Ir(*cod*)Cl]<sub>2</sub> (3 mol %)} and longer reaction time (6 d), we isolated the desired oxindole (+)-**4f** in 81% yield and 92% ee, along with recovery of the HypPhos **2** in 82% yield. Crystallization of (+)-**4f** from cyclohexane and EtOAc yielded higher enantiopurity (97% ee), with X-ray crystallography confirming the absolute configuration to be *S*.<sup>26,29,31</sup> The potential utility of this method was further illustrated through the syntheses of several alkaloid targets (Schemes 1B–D). Reduction of (+)-**4f** with DIBAL-H afforded (+)-**12** in 83% yield (Scheme 1B). After TBS protection, the Fischer indole reaction catalyzed by ZnCl<sub>2</sub> yielded (+)-**13**, a key intermediate in the synthesis of gliocladin C,<sup>32,33</sup> in 90% yield, completing the formal synthesis of (–)-gliocladin C. Gliocladin C is a known precursor of gliocladine C.<sup>32b</sup> Notably, the activity of (–)-gliocladine C (IC<sub>50</sub>: 0.35 μM) against melanoma (A2508) cell lines is better than that of natural (+)-gliocladine C (IC<sub>50</sub>: 0.68 μM).<sup>32c</sup> Treatment of (+)-**12** with MsCl and NEt<sub>3</sub> gave (+)-**14** in 91% yield (Scheme 1C). Deprotection of the dimethoxy acetal group, using In(OTf)<sub>3</sub> in acetone, followed by reductive amination and spontaneous cyclization furnished (–)-coerulescine in 64% yield.<sup>34</sup> A two-step protocol has been reported previously for the preparation of horsfiline from coerulescine,<sup>34d</sup> allowing us to claim a formal synthesis of (–)-horsfiline. Methylation of (+)-**14**, reduction of the mesylate with NaBH<sub>4</sub>, followed by deprotection of the dimethoxy acetal group afforded (–)-**15** in 54% overall yield (Scheme 1D). Formation of the imine with MeNH<sub>2</sub> and MgSO<sub>4</sub> followed by in situ reduction with LiAlH<sub>4</sub> and cyclization furnished (+)-deoxyeseroline in 81% yield. Following the reported procedure,<sup>16c,35</sup> (+)-deoxyeseroline could be used to prepare (+)-esermethole and (+)-physostigmine. Interestingly, (–)-physostigmine is clinically useful as an anticholinergic drug for Alzheimer's disease, whereas its enantiomer (+)-physostigmine is not, but it has been used experimentally to protect animals from organophosphate poisoning.<sup>36</sup> Treatment of (–)-**15** with LiAlH<sub>4</sub> gave the aminal (+)-**16**, a known precursor of (+)-physovenine.<sup>37</sup>

We used density functional theory (DFT) calculations to elucidate the reaction mechanism and origin of enantioselectivity of the asymmetric Staudinger–aza-Wittig reaction (see the SI for computational details). We investigated the reaction of the Lewis acid-bound iminophosphorane **17** derived from the chiral phosphine **2** and the malonate **3a** in the presence of phenylsilane as the reductant and [Ir(*cod*)Cl]<sub>2</sub> as the Lewis acid (Figure 2A).<sup>38</sup> From **17**, the concerted [2 + 2] cycloaddition (**TS1**) gives the oxazaphosphetane

intermediate **18** followed by stepwise retro-[2 + 2] cycloaddition<sup>39</sup> to cleave the P–N and C–O bonds sequentially, via transition states **TS2** and **TS3**, respectively. Because both of the enantiotopic malonate ester groups might have reacted with the two different  $\pi$ -faces of the PN bonds in the *cis* and *trans* isomers of the iminophosphorane, we considered all eight of these possible stereoisomeric pathways (pathways **A–H**). Figure 2A presents the reaction energy profiles of the two most favorable pathways (**A** and **B**) leading to the (*S*)- and (*R*)-enantiomers of the product (**11** and **ent-11**, respectively; see Figures S2–S5 for the less favorable pathways). In the rate- and enantioselectivity-determining P–N bond cleavage step (**TS2**), pathway **A** leading to the major enantiomeric product **11** has an activation barrier 2.5 kcal/mol lower than that of pathway **B** leading to **ent-11**, consistent with the high ee we observed experimentally (93% ee). In pathway **A**, the rate-determining transition state for retro-[2 + 2] cycloaddition (**TS2-A**) is stabilized by [C–H $\cdots\pi$ ] interactions between the 7-OTBS group on HypPhos and the benzene ring on the substrate (Figure 2B). The computed geometry of **TS2-A** features a Me group on the OTBS unit positioned optimally from the benzene ring on the substrate (3.10 Å) to form a stabilizing [C–H $\cdots\pi$ ] interaction, rather than a repulsive one.<sup>40</sup> On the other hand, in **TS2-B**, the bulky *tert*-butoxy unit, rather than the benzene ring, is positioned toward the bicyclic framework of the HypPhos scaffold, leading to unfavorable steric interactions between the *tert*-butoxy and HypPhos units.

Next, we investigated how the Lewis acid affected the reactivity and enantioselectivity. For the reaction of the iminophosphorane **21** in the absence of a Lewis acid, our calculations indicate that the [2 + 2] and retro-[2 + 2] cycloaddition steps both occur with higher activation barriers and that the computed enantioselectivity ( $\Delta G^\ddagger = 0.4$  kcal/mol) is diminished (Figure 2C). These findings are consistent with the lower reactivity and enantioselectivity we observed experimentally in the absence of a Lewis acid (Table 1). The Lewis acid not only promotes the [2 + 2] cycloaddition by enhancing the nucleophilicity of the carbonyl group but also facilitates the retro-[2 + 2] cycloaddition step kinetically. In the absence of a Lewis acid, the retro-[2 + 2]-cycloaddition occurs in a concerted manner<sup>13</sup> with an activation barrier of 27.2 kcal/mol. When [Ir(*cod*)Cl]<sub>2</sub> was present, the retro-[2 + 2] cycloaddition occurs through a kinetically more favorable stepwise process in which the Lewis acid stabilizes the negative charge in the zwitterionic intermediate **19-A**.

## CONCLUSIONS

In conclusion, we have developed a phosphine oxide-catalyzed asymmetric Staudinger–aza-Wittig reaction of (*o*-azidoaryl)malonates, allowing access to a range of valuable chiral quaternary oxindoles. The reaction occurs under mild conditions, with good functional group tolerance, a wide substrate scope, and excellent enantioselectivity. The success of this reaction relies on the rationally designed HypPhos oxide **2•[O]** featuring a strained [2.2.1]-bicyclic core structure (facilitating P<sup>III</sup>/P<sup>V</sup>=O redox cycling) and steric bulk (avoiding “self-quenching” in the presence of Lewis acids {e.g., [Ir(*cod*)Cl]<sub>2</sub>}). The Ir<sup>I</sup> center acts as a Lewis acid in this process, promoting the aza-Wittig reaction of relatively inert malonates and assisting the P<sup>III</sup>/P<sup>V</sup>=O redox cycling in the presence of phenylsilane as the reductant. Through DFT-based calculations, we elucidated the origin of the enantioselectivity and highlighted the cooperative effects of the Ir<sup>I</sup> center and our



designed HypPhos in facilitating the desymmetrization. Moreover, we highlight the utility of this methodology through (formal) syntheses of seven alkaloid targets: (–)-gliocladin C, (–)-coerulescine, (–)-horsfiline, (+)-deoxyeseroline, (+)-esermethole, (+)-physostigmine, and (+)-physovenine.

## Supplementary Material

Refer to Web version on PubMed Central for supplementary material.

## ACKNOWLEDGMENTS

Financial support for this study was provided by the NIH (R01GM071779 to O.K.; R35GM128779 to P.L.). We thank the UCLA Molecular Instrumentation Center for providing the instrumentation for NMR spectroscopy and mass spectrometry; Dr. Saeed Khan (UCLA) for the crystallographic analyses, and Andrew Kelleghan and Prof. Neil K. Garg (UCLA) for sharing their SFC instrument. DFT calculations were performed at the Center for Research Computing at the University of Pittsburgh (H2P cluster; supported by NSF award number OAC-2117681) and the Extreme Science and Engineering Discovery Environment (XSEDE; supported by NSF grant number ACI-1548562).

## REFERENCES

- (1). For reviews on Wittig reactions, see:(a)Heravi MM; Zadsirjan V; Hamidi H; Daraie M; Momeni T Recent Applications of the Wittig Reaction in Alkaloid Synthesis. In *The Alkaloids: Chemistry and Biology*; Knölker, H. J, Ed.; Academic Press: San Diego, 2020; Vol. 84, pp. 201–334. (b)Heravi MM; Zadsirjan V; Daraie M; Ghanbarian M Applications of Wittig Reaction in the Total Synthesis of Natural Macrolides. *ChemistrySelect* 2020, 5, 9654–9690.(c)Hoffmann RW Wittig and His Accomplishments: Still Relevant Beyond His 100<sup>th</sup> Birthday. *Angew. Chem., Int. Ed.* 2001, 40, 1411–1416.(d)Maryanoff BE; Reitz AB The Wittig Olefination Reaction and Modifications Involving Phosphoryl-Stabilized Carbanions. *Stereochemistry, Mechanism, and Selected Synthetic Aspects. Chem. Rev.* 1989, 89, 863–927.
- (2). For reviews on Staudinger-type reactions, see:(a)Pedroo K; Montazer MN; Larijani B; Mahdavi M Recent Advances in the Synthesis of Heterocycles by the Aza-Wittig Reaction. *Synthesis* 2021, 53, 2342–2366.(b)Palacios F; Alonso C; Aparicio D; Rubiales G; de los Santos JM Aza-Wittig Reaction in Natural Product Syntheses. In *Organic Azides*; John Wiley & Sons: Hoboken, NJ, 2009; pp. 437–467.(c)Palacios F; Aparicio D; Rubiales G; Alonso C; de los Santos JM Synthetic Applications of Intramolecular Aza-Wittig Reaction for the Preparation of Heterocyclic Compounds. *Curr. Org. Chem.* 2009, 13, 810.(d)Palacios F; Alonso C; Aparicio D; Rubiales G; de los Santos JM The Aza-Wittig Reaction: An Efficient Tool for the Construction of Carbon–Nitrogen Double Bonds. *Tetrahedron* 2007, 63, 523–575. (e)Guchi S Recent Progress in the Synthesis of Heterocyclic Natural Products by the Staudinger/Intramolecular Aza-Wittig Reaction. *ARKIVOC* 2005, 98.(f)Fresneda PM; Molina P Application of Iminophosphorane-Based Methodologies for the Synthesis of Natural Products. *Synlett* 2004, 1–17.(g)Wamhoff H; Richardt G; Stölben S Iminophosphoranes: Versatile Tools in Heterocyclic Synthesis. In *Advances in Heterocyclic Chemistry*; Katritzky, A. R, Ed.; Academic Press: San Diego, 1995; Vol. 64, pp. 159–249.(h)Gololobov YG; Kasukhin LF Recent Advances in the Staudinger Reaction. *Tetrahedron* 1992, 48, 1353–1406.(i)Gololobov YG; Zhmurova IN; Kasukhin LF Sixty Years of Staudinger Reaction. *Tetrahedron* 1981, 37, 437–472.
- (3). For reviews on reactions regarding catalytic cycling of phosphine oxides, see:(a)Xie C; Smaligo AJ; Song X-R; Kwon O Phosphorus-Based Catalysis. *ACS Cent. Sci.* 2021, 7, 536–558. [PubMed: 34056085] (b)Lipshultz JM; Li G; Radosevich AT Main Group Redox Catalysis of Organopnictogens: Vertical Periodic Trends and Emerging Opportunities in Group 15. *J. Am. Chem. Soc.* 2021, 143, 1699–1721. [PubMed: 33464903] (c)Guo H; Fan YC; Sun Z; Wu Y; Kwon O Phosphine Organocatalysis. *Chem. Rev.* 2018, 118, 10049–10293. [PubMed: 30260217] (d)Beddoe RH; Sneddon HF; Denton RM The Catalytic Mitsunobu Reaction: A Critical Analysis of the Current State-of-the-Art. *Org. Biomol. Chem.* 2018, 16, 7774. [PubMed: 30306184] (e)Lao Z; Toy PH Catalytic Wittig and Aza-Wittig Reactions. *Beilstein J. Org. Chem.* 2016, 12,

2577–2587. [PubMed: 28144327] (f)Marsden SP In Sustainable Catalysis; Dunn PJ, Hii KK, Krische MJ, Williams MT, Eds.; John Wiley & Sons: New York, 2013; pp. 339–361.(g)An J; Denton RM; Lambert TH; Nacsa ED The Development of Catalytic Nucleophilic Substitution Reactions: Challenges, Progress and Future Directions. *Org. Biomol. Chem.* 2014, 12, 2993–3003. [PubMed: 24699913] (h)Xu S; Tang Y Catalytic Approaches to Stoichiometric Phosphine-Mediated Organic Reactions. *Lett. Org. Chem.* 2014, 11, 524–533.(i)van Kalker HA; van Delft FL; Rutjes FPJT Organophosphorus Catalysis to Bypass Phosphine Oxide Waste. *ChemSusChem* 2013, 6, 1615–1624. [PubMed: 24039197]

- (4). For reviews on the reduction of phosphine oxides, see:(a)Hérault D; Nguyen DH; Nuel D; Buono G Reduction of Secondary and Tertiary Phosphine Oxides to Phosphines. *Chem. Soc. Rev.* 2015, 44, 2508–2528. [PubMed: 25714261] (b)Podyacheva E; Kuchuk E; Chusov D Reduction of Phosphine Oxides to Phosphines. *Tetrahedron Lett.* 2019, 60, 575–582.
- (5). For reviews on asymmetric Wittig-type reactions, see:(a)Rein T; Pedersen TM Asymmetric Wittig Type Reactions. *Synthesis* 2002, 579–594.(b)Zhang K; Lu L-Q; Xiao W-J Recent Advances in the Catalytic Asymmetric Alkylation of Stabilized Phosphorous Ylides. *Chem. Commun.* 2019, 55, 8716–8721.
- (6). Werner T; Hoffmann M; Deshmukh S First Enantioselective Catalytic Wittig Reaction. *Eur. J. Org. Chem.* 2014, 2014, 6630–6633.
- (7). (a)Schmiedel VM; Hong YJ; Lentz D; Tantillo DJ; Christmann M Synthesis and Structure Revision of Dichrocephones A and B. *Angew. Chem., Int. Ed.* 2018, 57, 2419–2422.(b)Schneider LM; Schmiedel VM; Pecchioli T; Lentz D; Merten C; Christmann M Asymmetric Synthesis of Carbocyclic Propellanes. *Org. Lett.* 2017, 19, 2310–2313. [PubMed: 28445060]
- (8). Lorton C; Castanheiro T; Voituriez A Catalytic and Asymmetric Process via P<sup>III</sup>/P<sup>V</sup>=O Redox Cycling: Access to (Trifluoromethyl)Cyclobutenes via a Michael Addition/Wittig Olefination Reaction. *J. Am. Chem. Soc.* 2019, 141, 10142–10147. [PubMed: 31194912]
- (9). Wilson SR; Pasternak A Preparation of a New Class of C<sub>2</sub>-Symmetric Chiral Phosphines: The First Asymmetric Staudinger Reaction. *Synlett* 1990, 199–200.
- (10). Lertpibulpanya D; Marsden SP; Rodriguez-Garcia I; Kilner CA Asymmetric Aza-Wittig Reactions: Enantioselective Synthesis of  $\beta$ -Quaternary Azacycles. *Angew. Chem., Int. Ed.* 2006, 45, 5000–5002.
- (11). (a)Kirk AM; O'Brien CJ; Krenske EH Why Do Silanes Reduce Electron-Rich Phosphine Oxides Faster than Electron-Poor Phosphine Oxides? *Chem. Commun.* 2020, 56, 1227–1230.(b)Zhang K; Cai L; Yang Z; Houk KN; Kwon O Bridged [2.2.1] Bicyclic Phosphine Oxide Facilitates Catalytic  $\gamma$ -Umpolung Addition–Wittig Olefination. *Chem. Sci.* 2018, 9, 1867–1872. [PubMed: 29732112]
- (12). Examples of redox cycling of phosphine oxides under mild conditions:(a)Longwitz L; Spannenberg A; Werner T Phosphetane Oxides as Redox Cycling Catalysts in the Catalytic Wittig Reaction at Room Temperature. *ACS Catal.* 2019, 9, 9237–9244.(b)Ghosh A; Lecomte M; Kim-Lee S-H; Radosevich AT Organophosphorus-Catalyzed Deoxygenation of Sulfonyl Chlorides: Electrophilic (Fluoroalkyl)Sulfonylation by P<sup>III</sup>/P<sup>V</sup>=O Redox Cycling. *Angew. Chem., Int. Ed.* 2019, 58, 2864–2869.(c)Zhao W; Yan PK; Radosevich AT A Phosphetane Catalyzes Deoxygenative Condensation of  $\alpha$ -Keto Esters and Carboxylic Acids via P<sup>III</sup>/P<sup>V</sup>=O Redox Cycling. *J. Am. Chem. Soc.* 2015, 137, 616–619. [PubMed: 25564133] (d)O'Brien CJ; Lavigne F; Coyle EE; Holohan AJ; Doonan BJ Breaking the Ring Through a Room Temperature Catalytic Wittig Reaction. *Chem. – Eur. J.* 2013, 19, 5854. [PubMed: 23526683]
- (13). Catalytic asymmetric aza-Wittig reaction:Cai L; Zhang K; Chen S; Lepage RJ; Houk KN; Krenske EH; Kwon O Catalytic Asymmetric Staudinger–Aza-Wittig Reaction for the Synthesis of Heterocyclic Amines. *J. Am. Chem. Soc.* 2019, 141, 9537–9542. [PubMed: 31184143]
- (14). (a)Khetmalis YM; Shivani M; Murugesan S; Chandra Sekhar KVG Oxindole and Its Derivatives: A Review on Recent Progress in Biological Activities. *Biomed. Pharmacother.* 2021, 141, 111842. [PubMed: 34174506] (b)Kaur M; Singh M; Chadha N; Silakari O Oxindole: A Chemical Prism Carrying Plethora of Therapeutic Benefits. *Eur. J. Med. Chem.* 2016, 123, 858–894. [PubMed: 27543880]
- (15). For reviews on oxindoles, see:(a)Boddy AJ; Bull JA Stereoselective Synthesis and Applications of Spirocyclic Oxindoles. *Org. Chem. Front.* 2021, 8, 1026–1084.(b)Marchese AD; Larin

- EM; Mirabi B; Lautens M Metal-Catalyzed Approaches Toward the Oxindole Core. *Acc. Chem. Res.* 2020, 53, 1605–1619. [PubMed: 32706589] (c)Cao Z-Y; Zhou F; Zhou J Development of Synthetic Methodologies via Catalytic Enantioselective Synthesis of 3,3-Disubstituted Oxindoles. *Acc. Chem. Res.* 2018, 51, 1443–1454. [PubMed: 29808678] (d)Dalpozzo R Recent Catalytic Asymmetric Syntheses of 3,3-Disubstituted Indolin-2-ones and 2,2-Disubstituted Indolin-3-ones. *Adv. Synth. Catal.* 2017, 359, 1772–1810. (e)Dalpozzo R Catalytic Asymmetric Synthesis of Hetero-Substituted Oxindoles. *Org. Chem. Front.* 2017, 4, 2063–2078. (f)Millemaggi A; Taylor RJK 3-Alkenyl-oxindoles: Natural Products, Pharmaceuticals, and Recent Synthetic Advances in Tandem/Telescoped Approaches. *Eur. J. Org. Chem.* 2010, 4527–4547. (g)Badillo JJ; Hanhan NV; Franz AK Enantioselective Synthesis of Substituted Oxindoles and Spirooxindoles With Applications in Drug Discovery. *Curr. Opin. Drug Discovery Dev.* 2010, 13, 758–776. (h)Trost BM; Brennan MK Asymmetric Syntheses of Oxindole and Indole Spirocyclic Alkaloid Natural Products. *Synthesis* 2009, 3003–3025. (i)Galliford CV; Scheidt KA Pyrrolidinyl-Spirooxindole Natural Products as Inspirations for the Development of Potential Therapeutic Agents. *Angew. Chem., Int. Ed.* 2007, 46, 8748–8758. (j)Dounay AB; Overman LE The Asymmetric Intramolecular Heck Reaction in Natural Product Total Synthesis. *Chem. Rev.* 2003, 103, 2945–2964. [PubMed: 12914487] (k)Marti C; Carreira EM Construction of Spiro[pyrrolidine-3,3'-oxindoles]: Recent Applications to the Synthesis of Oxindole Alkaloids. *Eur. J. Org. Chem.* 2003, 2209–2219.
- (16). Selected examples of Heck-type reactions: (a)Chen M; Wang X; Yang P; Kou X; Ren Z-H; Guan Z-H Palladium-Catalyzed Enantioselective Heck Carbonylation With a Monodentate Phosphoramidite Ligand: Asymmetric Synthesis of (+)-Physostigmine, (+)-Physoverine, and (+)-Folicanthine. *Angew. Chem., Int. Ed.* 2020, 59, 12199–12205. (b)Zhang Z-M; Xu B; Wu L; Zhou L; Ji D; Liu Y; Li Z; Zhang J Palladium/XuPhos-Catalyzed Enantioselective Carbiodination of Olefin-Tethered Aryl Iodides. *J. Am. Chem. Soc.* 2019, 141, 8110–8115. [PubMed: 31070918] (c)Pinto A; Jia Y; Neuville L; Zhu J Palladium-Catalyzed Enantioselective Domino Heck–Cyanation Sequence: Development and Application to the Total Synthesis of Esermethole and Physostigmine. *Chem. – Eur. J.* 2007, 13, 961–967. [PubMed: 17009368] (d)Busacca CA; Grossbach D; So RC; O'Brie EM; Spinelli EM Probing Electronic Effects in the Asymmetric Heck Reaction With the BIPI Ligands. *Org. Lett.* 2003, 5, 595–598. [PubMed: 12583778] (e)Ashimori A; Bachand B; Overman LE; Poon DJ Catalytic Asymmetric Synthesis of Quaternary Carbon Centers. Exploratory Investigations of Intramolecular Heck Reactions of (E)- $\alpha,\beta$ -Unsaturated 2-Haloanilides and Analogues To Form Enantioenriched Spirocyclic Products. *J. Am. Chem. Soc.* 1998, 120, 6477–6487. (f)Ashimori A; Matsuura T; Overman LE; Poon DJ Catalytic Asymmetric Synthesis of Either Enantiomer of Physostigmine. Formation of Quaternary Carbon Centers with High Enantioselection by Intramolecular Heck Reactions of (Z)-2-Butenylidene. *J. Org. Chem.* 1993, 58, 6949–6951. An example of cyanoamidation: (g)Yasui Y; Kamisaki H; Takemoto Y Enantioselective Synthesis of 3,3-Disubstituted Oxindoles Through Pd-Catalyzed Cyanoamidation. *Org. Lett.* 2008, 10, 3303–3306. Examples of Ni-catalyzed dicarbofunctionalization: [PubMed: 18582078] (h)Chen X-W; Yue J-P; Wang K; Gui Y-Y; Niu Y-N; Liu J; Ran C-K; Kong W; Zhou W-J; Yu D-G Nickel-Catalyzed Asymmetric Reductive Carbo-Carboxylation of Alkenes with CO<sub>2</sub>. *Angew. Chem., Int. Ed.* 2021, 60, 14068–14075. (i)Fan P; Lan Y; Zhang C; Wang C Nickel/Photo-Cocatalyzed Asymmetric Acyl-Carbonylation of Alkenes. *J. Am. Chem. Soc.* 2020, 142, 2180–2186. [PubMed: 31971787]
- (17). Selected examples on alkylation: (a)Ma S; Han X; Krishnan S; Virgil SC; Stoltz BM Catalytic Enantioselective Stereoablative Alkylation of 3-Halooxindoles: Facile Access to Oxindoles with C3 All-Carbon Quaternary Stereocenters. *Angew. Chem., Int. Ed.* 2009, 48, 8037–8041. (b)Lee TBK; Wong GSK Asymmetric Alkylation of Oxindoles: An Approach to the Total Synthesis of (–)-Physostigmine. *J. Org. Chem.* 1991, 56, 872–875. Example of Michael addition: (c)He R; Ding C; Maruoka K Phosphonium Salts as Chiral Phase-Transfer Catalysts: Asymmetric Michael and Mannich Reactions of 3-Aryloxindoles. *Angew. Chem., Int. Ed.* 2009, 48, 4559–4561. An example of Claisen rearrangement: (d)Linton EC; Kozłowski MC Catalytic Enantioselective Meerwein–Eschenmoser Claisen Rearrangement: Asymmetric Synthesis of Allyl Oxindoles. *J. Am. Chem. Soc.* 2008, 130, 16162–16163. An example of a Mannich reaction: [PubMed: 18998679] (e)Tian X; Jiang K; Peng J; Du W; Chen Y-C Organocatalytic Stereoselective Mannich Reaction of 3-Substituted Oxindoles. *Org. Lett.* 2008, 10, 3583–3586. An example of an aldol reaction: [PubMed: 18642826] (f)Ogawa S; Shibata N; Inagaki J; Nakamura S;

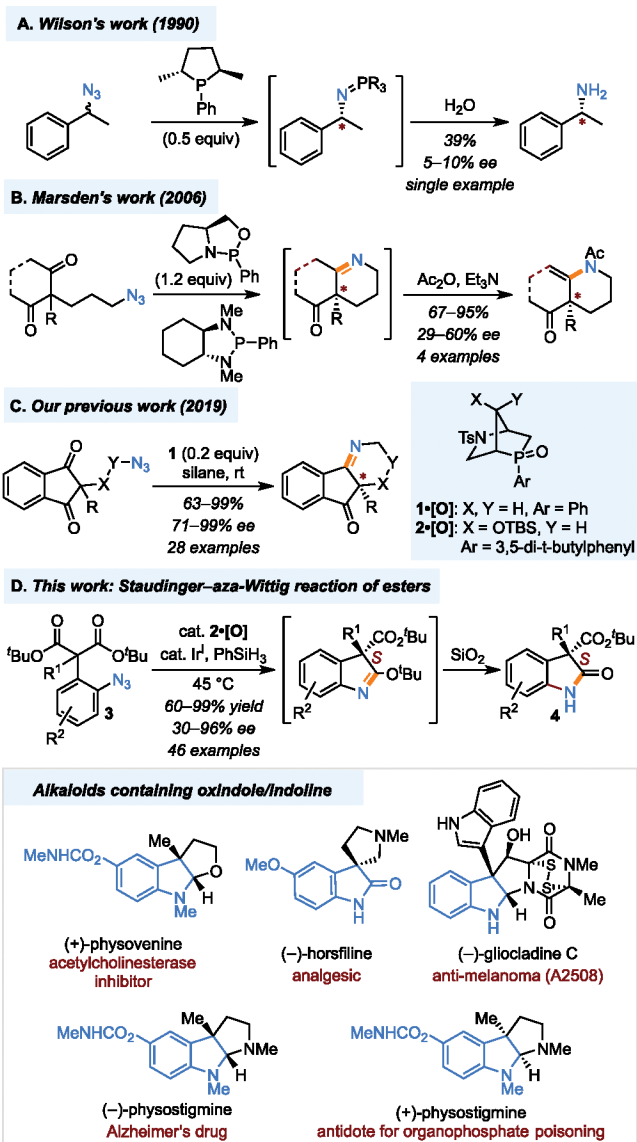
- Toru T; Shiro M Cinchona-Alkaloid-Catalyzed Enantioselective Direct Aldol-Type Reaction of Oxindoles with Ethyl Trifluoropyruvate. *Angew. Chem., Int. Ed.* 2007, 46, 8666–8669.
- An example of an allylation reaction:(g)Trost BM; Frederiksen MU Palladium-Catalyzed Asymmetric Allylation of Prochiral Nucleophiles: Synthesis of 3-Allyl-3-Aryl Oxindoles. *Angew. Chem., Int. Ed.* 2005, 44, 308–310. Examples of acyl-migration:(h)Hills ID; Fu GC Catalytic Enantioselective Synthesis of Oxindoles and Benzofuranones That Bear a Quaternary Stereocenter. *Angew. Chem., Int. Ed.* 2003, 42, 3921–3924.(i)Shaw SA; Aleman P; Vedejs E Development of Chiral Nucleophilic Pyridine Catalysts: Applications in Asymmetric Quaternary Carbon Synthesis. *J. Am. Chem. Soc.* 2003, 125, 13368–13369. [PubMed: 14583027]
- (18). Zeng X-P; Cao Z-Y; Wang Y-H; Zhou F; Zhou J Catalytic Enantioselective Desymmetrization Reactions to All-Carbon Quaternary Stereocenters. *Chem. Rev.* 2016, 116, 7330–7396. [PubMed: 27251100]
- (19). In a recent desymmetrization method using chiral phosphoric acid-catalyzed lactamization to prepare chiral oxindoles, the ee's ranged from 5 to 66%; see: Sumiyoshi T; Ishida K; Shimizu M; Yamai Y; Natsutani I; Uesato S; Nagaoka Y Asymmetric Synthesis of t-Butyl 3-Alkyl-Oxindole-3-Carboxylates via Chiral Phosphoric Acid Catalyzed Desymmetrization of Di-t-Butyl 2-Alkyl-2-(2-Aminophenyl)Malonates. *Heterocycles* 2019, 99, 1398–1411.
- (20). Examples of Staudinger-aza-Wittig reactions of esters:(a)Luo Z; Peplowski K; Sulikowski GA Formation of the BC Ring System of Upenamide via a Staudinger/Aza-Wittig Reaction. *Org. Lett.* 2007, 9, 5051–5054. [PubMed: 17973484] (b)Takeuchi H; Hagiwara S; Eguchi S A New Efficient Synthesis of Imidazolinones and Quinazolinone by Intramolecular Aza-Wittig Reaction. *Tetrahedron* 1989, 45, 6375–6386.
- (21). Examples of catalytic Staudinger-aza-Wittig reactions of esters:(a)Ren Z-L; Liu J-C; Ding M-W A Facile Synthesis of 4-Tetrazolyl-Substituted 4H-3,1-Benzoxazines Through Sequential Passerini-Azide/Acylation/Catalytic Aza-Wittig Reaction. *Synthesis* 2017, 49, 745.(b)Wang L; Xie Y-B; Huang N-Y; Yan J-Y; Hu W-M; Liu M-G; Ding M-W Catalytic Aza-Wittig Reaction of Acid Anhydride for the Synthesis of 4H-Benzo[d][1,3]Oxazin-4-Ones and 4-Benzylidene-2-Aryloxazol-5(4H)-Ones. *ACS Catal.* 2016, 6, 4010–4016.(c)van Kalkeren HA; te Grotenhuis C; Haasjes FS; Hommersom C(R)A; Rutjes FPJT; van Delft FL Catalytic Staudinger/Aza-Wittig Sequence by In Situ Phosphane Oxide Reduction. *Eur. J. Org. Chem.* 2013, 2013, 7059–7066.
- (22). García-Garrido SE; Presa Soto A; García-Álvarez J Chapter Three Iminophosphoranes (R<sub>3</sub>PNR'): From Terminal to Multidentate Ligands in Organometallic Chemistry. In *Advances in Organometallic Chemistry*; Pérez PJ, Ed.; 40 Years of GEQORSEQ; Academic Press: San Diego, 2022; Vol. 77, pp. 105–168.
- (23). Selected examples:(a)Buck E; Song ZJ; Tschaen D; Dormer PG; Volante RP; Reider PJ Ullmann Diaryl Ether Synthesis: Rate Acceleration by 2,2,6,6-Tetramethylheptane-3,5-dione. *Org. Lett.* 2002, 4, 1623–1626. [PubMed: 11975644] (b)Shafir A; Buchwald SL Highly Selective Room-Temperature Copper-Catalyzed C–N Coupling Reactions. *J. Am. Chem. Soc.* 2006, 128, 8742–8743. [PubMed: 16819863] (c)Cui X; Li J; Liu L; Guo QX 1,3-Dicarbonyl Compounds as Phosphine-Free Ligands for Pd-Catalyzed Heck and Suzuki Reactions. *Chin. Chem. Lett.* 2007, 18, 625–628.
- (24). Li Y; Das S; Zhou S; Junge K; Beller M General and Selective Copper-Catalyzed Reduction of Tertiary and Secondary Phosphine Oxides: Convenient Synthesis of Phosphines. *J. Am. Chem. Soc.* 2012, 134, 9727–9732. [PubMed: 22480270]
- (25). Henry CE; Xu Q; Fan YC; Martin TJ; Belding L; Dudding R; Kwon O Hydroxyproline-Derived Pseudoenantiomeric [2.2.1] Bicyclic Phosphines: Asymmetric Synthesis of (+)- and (–)-Pyrrolines. *J. Am. Chem. Soc.* 2014, 136, 11890–11893. [PubMed: 25099350]
- (26). See the Supporting Information for details.
- (27). Allen AE; MacMillan DWC Synergistic Catalysis: A Powerful Synthetic Strategy for New Reaction Development. *Chem. Sci.* 2012, 3, 633–658.
- (28). Without TBABF<sub>4</sub>, the reaction is very slow. For examples of ion exchange facilitated by TBABF<sub>4</sub>, see:(a)Takahashi T; Ogasawara S; Shinozaki Y; Tamiaki H Synthesis of Cationic Pyridinium–Chlorin Conjugates with Various Counter Anions and Effects of the Anions on Their Photophysical Properties. *Bull. Chem. Soc. Jpn.* 2020, 93, 467–476.(b)Kuyuldar S; Burda C; Connick WB Halide Exchange Studies of Novel Pd(II) NNN-Pincer Complexes. *RSC Adv.*



- 2019, 9, 25703–25711. [PubMed: 35530079] (c)Voloshin YZ; Varzatskii OA; Kron TE; Belsky VK; Zavodnik VE; Strizhakova NG; Palchik AV Triribbed-Functionalized Clathrochelate Iron(II) Dioximates as a New and Promising Tool To Obtain Polynucleating and Polynuclear Compounds With Improved Properties. *Inorg. Chem.* 2000, 39, 1907–1918. [PubMed: 11428111]
- (29). Our compound (+)-4n: [ $\alpha$ ]D<sub>25</sub> +138.0 (CHCl<sub>3</sub>, c = 0.50); known compound with R configuration (–)-4n: [ $\alpha$ ]D<sub>25</sub> –148.4 (CHCl<sub>3</sub>, c = 0.50), see: Hong S; Lee J; Kim M; Park Y; Park C; Kim M; Jew S; Park H Highly Enantioselective Synthesis of  $\alpha,\alpha$ -Dialkylmalonates by Phase-Transfer Catalytic Desymmetrization. *J. Am. Chem. Soc.* 2011, 133, 4924–4929. The other oxindoles were tentatively assigned to have the S configuration. [PubMed: 21388212]
- (30). (a)Schilling CI; Jung N; Biskup M; Schepers U; Bräse S Bioconjugation via Azide–Staudinger Ligation: An Overview. *Chem. Soc. Rev.* 2011, 40, 4840–4871. [PubMed: 21687844] (b)Lin FL; Hoyt HM; van Halbeek H; Bergman RG; Bertozzi CR Mechanistic Investigation of the Staudinger Ligation. *J. Am. Chem. Soc.* 2005, 127, 2686–2695. [PubMed: 15725026] (c)Saxon E; Armstrong JI; Bertozzi CRA “Traceless” Staudinger Ligation for the Chemoselective Synthesis of Amide Bonds. *Org. Lett.* 2000, 2, 2141–2143. [PubMed: 10891251]
- (31). The absolute Flack parameter was refined very close to zero [0.059(17)], indicating that the absolute configuration was as shown (S).
- (32). (a)Hajra S; Maity S; Maity R Efficient Synthesis of 3,3'-Mixed Bisindoles via Lewis Acid Catalyzed Reaction of Spiro-Epoxyoxindoles and Indoles. *Org. Lett.* 2015, 17, 3430–3433. [PubMed: 26158390] (b)DeLorbe JE; Horne D; Jove R; Mennen SM; Nam S; Zhang F-L; Overman LE General Approach for Preparing Epidithiodioxopiperazines From Trioxopiperazine Precursors: Enantioselective Total Syntheses of (+)- and (–)-Gliocladiene C, (+)-Leptosin D, (+)-T988C, (+)-Bionectin A, and (+)-Gliocladin A. *J. Am. Chem. Soc.* 2013, 135, 4117–4128. [PubMed: 23452236] (c)DeLorbe JE; Jabri SY; Mennen SM; Overman LE; Zhang F-L Enantioselective Total Synthesis of (+)-Gliocladiene C: Convergent Construction of Cyclotryptamine-Fused Polyoxopiperazines and a General Approach for Preparing Epidithiodioxopiperazines From Trioxopiperazine Precursors. *J. Am. Chem. Soc.* 2011, 133, 6549–6552. [PubMed: 21473649]
- (33). Other enantioselective syntheses of Gliocladin C:(a)Tayu M; Hui Y; Takeda S; Higuchi K; Saito N; Kawasaki T Total Synthesis of (+)-Gliocladin C Based on One-Pot Construction of a 3a-(3-Indolyl)Pyrroloindoline Skeleton by Sulfonium-Mediated Cross-Coupling of Tryptophan and Indole. *Org. Lett.* 2017, 19, 6582–6585. [PubMed: 29205043] (b)Lei H; Wang L; Xu Z; Ye T Regio- and Stereospecific Construction of 3a-(1H-Indol-3-yl)pyrrolidinoindolines and Application to the Formal Syntheses of Gliocladins B and C. *Org. Lett.* 2017, 19, 5134–5137. [PubMed: 28920696] (c)Zhu G; Bao G; Li Y; Sun W; Li J; Hong L; Wang R Efficient Catalytic Kinetic Resolution of Spiro-Epoxyoxindoles with Concomitant Asymmetric Friedel–Crafts Alkylation of Indoles. *Angew. Chem., Int. Ed.* 2017, 56, 5332–5335.(d)Huang J-Z; Wu X; Gong L-Z Enantioselective Organocatalytic Addition of Nitroalkanes to Oxindolylideneindolenines for the Construction of Chiral 3,3-Disubstituted Oxindoles. *Adv. Synth. Catal.* 2013, 355, 2531–2537.(e)Song J; Guo C; Adele A; Yin H; Gong L-Z Enantioselective Organocatalytic Construction of Hexahydropyrroloindole by Means of  $\alpha$ -Alkylation of Aldehydes Leading to the Total Synthesis of (+)-Gliocladin C. *Chem. – Eur. J.* 2013, 19, 3319–3323. [PubMed: 23401076] (f)Sun M; Hao X-Y; Liu S; Hao X-J Formal Synthesis of (+)-Gliocladin C. *Tetrahedron Lett.* 2013, 54, 692–694.(g)Boyer N; Movassaghi M Concise Total Synthesis of (+)-Gliocladins B and C. *Chem. Sci.* 2012, 3, 1798–1803. [PubMed: 22844577] (h)Furst L; Narayanam JMR; Stephenson CRJ Total Synthesis of (+)-Gliocladin C Enabled by Visible-Light Photoredox Catalysis. *Angew. Chem., Int. Ed.* 2011, 50, 9655–9659.(i)Overman LE; Shin Y Enantioselective Total Synthesis of (+)-Gliocladin C. *Org. Lett.* 2007, 9, 339–341. [PubMed: 17217299]
- (34). Isolation of (–)-coerulescine:(a)Anderton N; Cockrum PA; Colegate SM; Edgar JA; Flower K; Vit I; Willing RI Oxindoles from *Phalaris coerulescens*. *Phytochemistry* 1998, 48, 437–439. Enantioselective syntheses of coerulescine:(b)Sathish M; Nachtigall FM; Santos LS Bifunctional Thiosquaramide Catalyzed Asymmetric Reduction of Dihydro- $\beta$ -Carbolines and Enantioselective Synthesis of (–)-Coerulescine and (–)-Horsfiline by Oxidative Rearrangement. *RSC Adv.* 2020, 10, 38672–38677. [PubMed: 35517527] (c)Lee S; Yang J; Yang S; Lee G; Oh D; Ha MW; Hong S; Park H Enantioselective Synthesis of (+)-Coerulescine by a Phase-Transfer Catalytic Allylation of Diphenylmethyl tert-Butyl  $\alpha$ -(2-Nitrophenyl)Malonate. *Front. Chem.* 2020, 8,

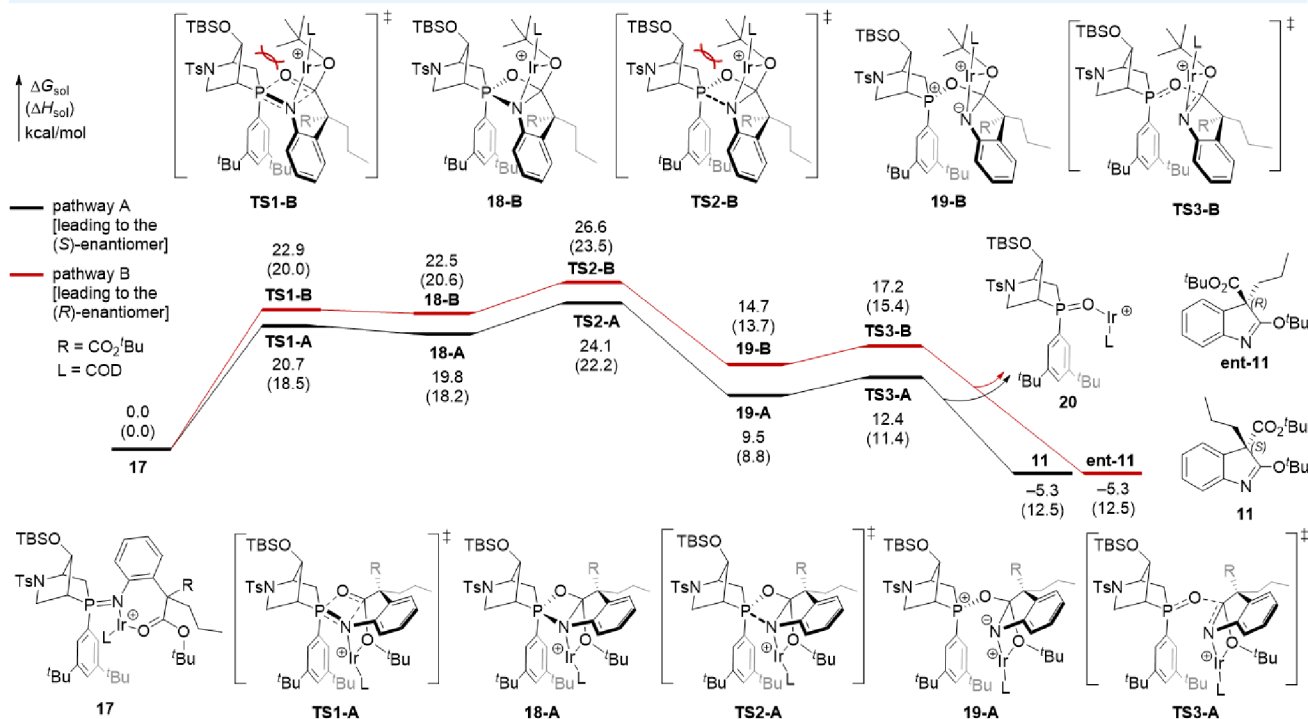
- 5773718.(d)De S; Das MK; Bhunia S; Bisai A Unified Approach to the Spiro(Pyrrolidinyl-Oxindole) and Hexahydropyrrolo[2,3-b]Indole Alkaloids: Total Syntheses of Pseudophrynamines 270 and 272A. *Org. Lett.* 2015, 17, 5922–5925. [PubMed: 26600374] (e)Mukaiyama T; Ogata K; Sato I; Hayashi Y Asymmetric Organocatalyzed Michael Addition of Nitromethane to a 2-Oxindoline-3-Ylidene Acetaldehyde and the Three One-Pot Sequential Synthesis of (–)-Horsfiline and (–)-Coerulescine. *Chem. – Eur. J.* 2014, 20, 13583–13588. [PubMed: 25155110] (f)Shen K; Liu X; Wang W; Wang G; Cao W; Li W; Hu X; Lin L; Feng X Highly Enantioselective Synthesis of 1,3-Bis(hydroxymethyl)-2-oxindoles from Unprotected Oxindoles and Formalin Using a Chiral NdIII Complex. *Chem. Sci.* 2010, 1, 590–595.(g)Li C; Chan C; Heimann AC; Danishefsky SJ On the Rearrangement of an Azaspiroindolenine to a Precursor to Phalarine: Mechanistic Insights. *Angew. Chem., Int. Ed.* 2007, 46, 1444–1447.
- (35). Kong W; Wang Q; Zhu J Palladium-Catalyzed Enantioselective Domino Heck/Intermolecular C–H Bond Functionalization: Development and Application to the Synthesis of (+)-Esermethole. *J. Am. Chem. Soc.* 2015, 137, 16028–16031. [PubMed: 26681502]
- (36). Greig NH; Pei X-F; Soncrant TT; Ingram DK; Bossi A Phenserine and Ring C Hetero-Analogues: Drug Candidates for the Treatment of Alzheimer’s Disease. *Med. Res. Rev.* 1995, 15, 3–31. [PubMed: 7898167]
- (37). Kulkarni MG; Dhondge AP; Borhade AS; Gaikwad DD; Chavhan SW; Shaikh YB; Nigdale VB; Desai MP; Birhade DR; Shinde MP Total Synthesis of (±)-Physovenine. *Eur. J. Org. Chem.* 2009, 3875–3877.
- (38). Our DFT calculations indicate that the binding of the Ir-based Lewis acid to 21 to generate a Lewis acid–bound iminophosphorane is exergonic by 3.9 kcal/mol (see the SI for details).
- (39). A previous study suggests that Lewis acid–catalyzed carbonylolefin metathesis with styrene-derived substrates favors a stepwise retro-[2+2] cycloaddition mechanism: Ludwig JR; Phan S; McAtee CC; Zimmerman PM; Devery JJ; Schindler CS Mechanistic Investigations of the Iron(III)-Catalyzed Carbonyl-Olefin Metathesis Reaction. *J. Am. Chem. Soc.* 2017, 139, 10832–10842. [PubMed: 28753008]
- (40). (a)Fanourakis A; Docherty PJ; Chuentragool P; Phipps RJ Recent Developments in Enantioselective Transition Metal Catalysis Featuring Attractive Noncovalent Interactions between Ligand and Substrate. *ACS Catal.* 2020, 10, 10672–10714. [PubMed: 32983588] (b)Ringer AL; Figs MS; Sinnokrot MO; Sherrill CD Aliphatic C–H/ $\pi$  interactions: Methane–Benzene, Methane–Phenol, and Methane–Indole Complexes. *J. Phys. Chem. A* 2006, 110, 10822–10828. [PubMed: 16970377] (c)Tsuzuki S; Honda K; Uchimaru T; Mikami M; Fujii A Magnitude and Directionality of the Interaction Energy of the Aliphatic CH/ $\pi$  Interaction: Significant Difference From Hydrogen Bond. *J. Phys. Chem. A* 2006, 110, 10163–10168. [PubMed: 16913692]



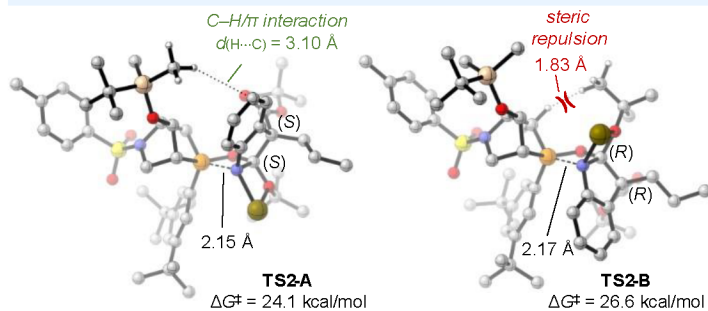


**Figure 1.**  
Asymmetric Staudinger processes.

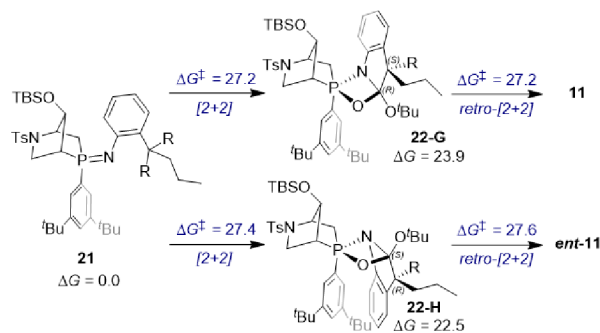
**A. Reaction energy profile of the asymmetric Staudinger–aza-Wittig reaction of Lewis acid-bound iminophosphorane 17 derived from 2 and 3a**



**B. Rate- and enantioselectivity-determining retro-[2+2]-cycloaddition transition states†**



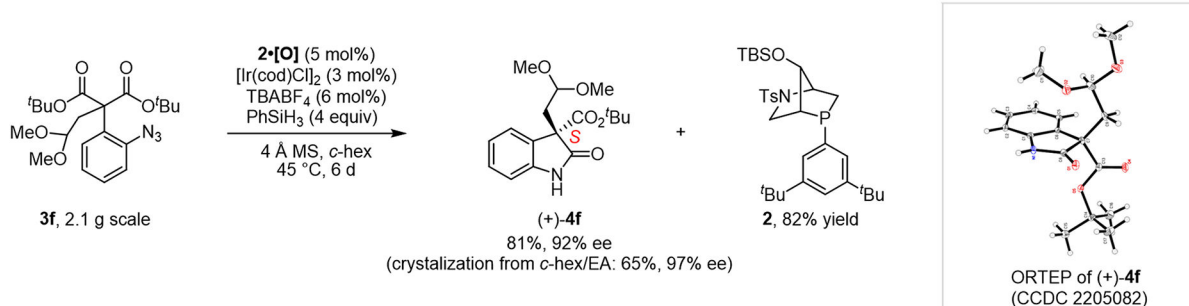
**C. Reaction of iminophosphorane 21 in the absence of Lewis acid**



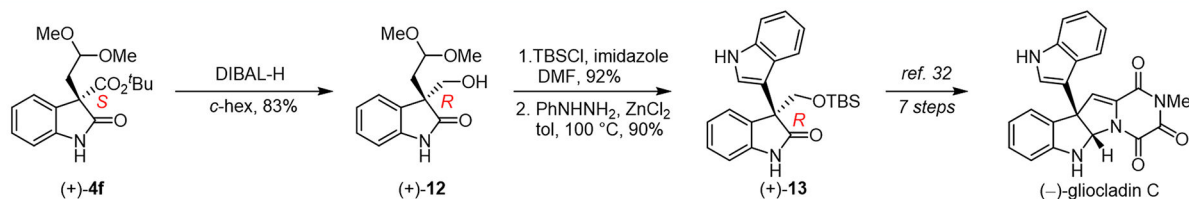
**Figure 2.**

Computational study of the mechanism, origin of enantioselectivity, and effect of the Lewis acid of the asymmetric Staudinger–aza-Wittig reaction. All Gibbs free energies and enthalpies (in kcal/mol) were computed at the  $\omega$ B97X-D/6-311 + G(d,p)–SDD(Ir)/SMD(cyclohexane)//B3LYP-D3/6-31G(d)–SDD(Ir) level of theory.

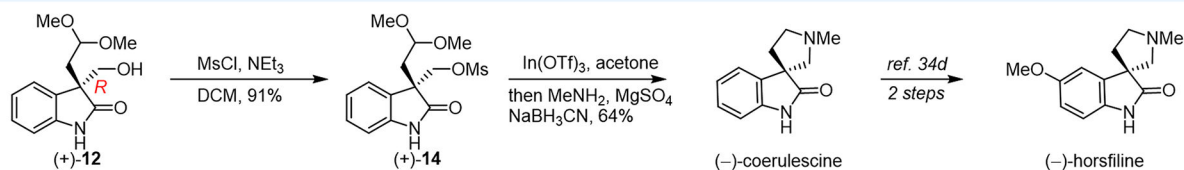
## A. Scale-up asymmetric Staudinger–aza-Wittig reaction



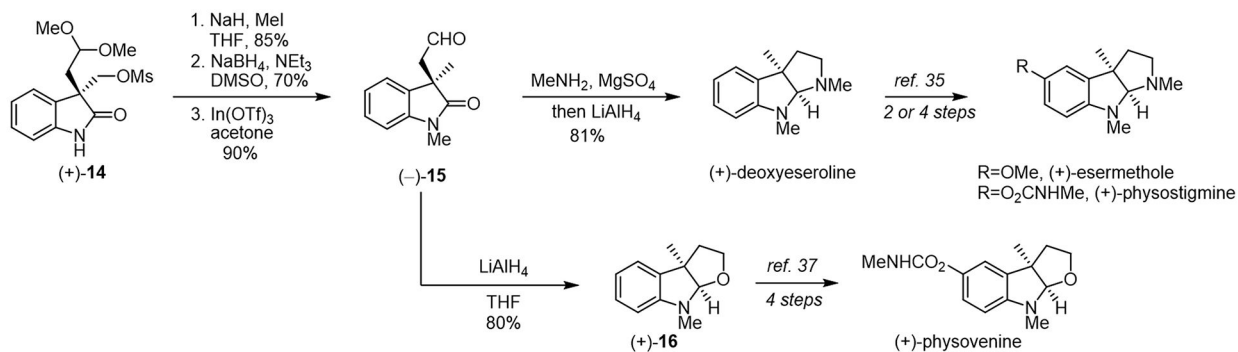
## B. Formal synthesis of (–)-gliocladin C



## C. Synthesis of (–)-coerulescine and formal synthesis of (–)-horsfiline

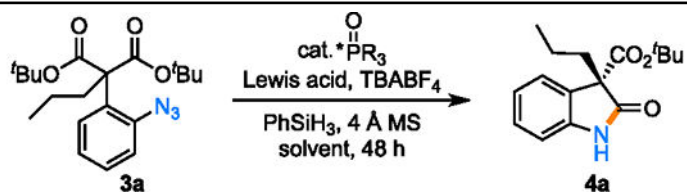


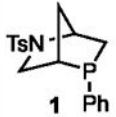
## D. Synthesis of (+)-deoxyeseroline and formal synthesis of (+)-esermethole, (+)-physostigmine and (+)-physovenine



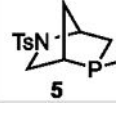
**Scheme 1.**  
Scaled-up Staudinger–aza-Wittig Reaction and Synthetic Applications

Table 1.

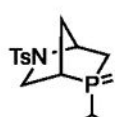
Optimization of Reaction Conditions<sup>a,i</sup>




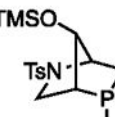
**1**



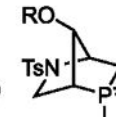
**5**



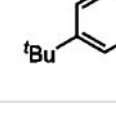
**6•[O]**



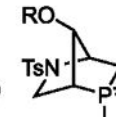
**7•[O]**



**8•[O]**



**9•[O]**



**10•[O]**

**2•[O]** R = TBS  
**8•[O]** R = TMS  
**9•[O]** R = TES  
**10•[O]** R = TIPS

| entry              | *PR <sub>3</sub> (mol %) | Lewis acid (mol%)                      | solvent                 | T (°C) | yield <sup>b</sup> (%) | ee <sup>c</sup> (%) |
|--------------------|--------------------------|--|-------------------------|--------|------------------------|---------------------|
| 1 <sup>d,e,f</sup> | 1 (100)                  |  | tol                     | 70     | 95                     | 58                  |
| 2 <sup>d,e,f</sup> | 5 (100)                  |  | tol                     | 70     | 85                     | 11                  |
| 3 <sup>d,e,f</sup> | 1 (100)                  |  | tol                     | 40     | trace                  | n.d.                |
| 4 <sup>f</sup>     | 1•[O] (20)               | CuF <sub>2</sub> (20)                  | tol                     | 35     | 81                     | 78                  |
| 5 <sup>f</sup>     | 1•[O] (20)               | CuF <sub>2</sub> (20)                  | <i>c</i> -hex           | 35     | 50                     | 82                  |
| 6 <sup>f</sup>     | 6•[O] (20)               | CuF <sub>2</sub> (20)                  | <i>c</i> -hex           | 35     | 92                     | 77                  |
| 7 <sup>f</sup>     | 7•[O] (20)               | CuF <sub>2</sub> (20)                  | <i>c</i> -hex           | 35     | 30                     | 89                  |
| 8 <sup>f</sup>     | 8•[O] (20)               | CuF <sub>2</sub> (20)                  | <i>c</i> -hex           | 35     | 95                     | 87                  |
| 9                  | 8•[O] (20)               | [Ir( <i>cod</i> )Cl] <sub>2</sub> (10) | <i>c</i> -hex/tol (1:1) | 35     | 95                     | 92                  |
| 10                 | 8•[O] (10)               | [Ir( <i>cod</i> )Cl] <sub>2</sub> (5)  | <i>c</i> -hex           | 45     | 95                     | 93                  |
| 11                 | 9•[O] (10)               | [Ir( <i>cod</i> )Cl] <sub>2</sub> (5)  | <i>c</i> -hex           | 45     | 98                     | 92                  |
| 12                 | 2•[O] (10)               | [Ir( <i>cod</i> )Cl] <sub>2</sub> (5)  | <i>c</i> -hex           | 45     | 96                     | 93                  |
| 13                 | 10•[O] (10)              | [Ir( <i>cod</i> )Cl] <sub>2</sub> (5)  | <i>c</i> -hex           | 45     | 88                     | 88                  |
| 14 <sup>g</sup>    | 2•[O] (10)               | [Ir( <i>cod</i> )Cl] <sub>2</sub> (5)  | <i>c</i> -hex           | 45     | 98                     | 93                  |
| 15 <sup>h</sup>    | 2•[O] (10)               | [Ir( <i>cod</i> )Cl] <sub>2</sub> (5)  | <i>c</i> -hex           | 45     | 92                     | 92                  |

<sup>a</sup>Reactions performed on a 0.05 mmol scale with 4.0 equiv of PhSiH<sub>3</sub>, unless otherwise noted.<sup>b</sup>Isolated yield.<sup>c</sup>Enantiomeric excess (ee) determined using chiral-phase HPLC.<sup>d</sup>No PhSiH<sub>3</sub>.<sup>e</sup>No 4 Å molecular sieves.<sup>f</sup>No TBABF<sub>4</sub>.

<sup>g</sup>PhSiH<sub>3</sub>: 3 equiv.

<sup>h</sup>PhSiH<sub>3</sub>: 2 equiv.

<sup>i</sup>TBABF<sub>4</sub>: tetrabutylammonium tetrafluoroborate; tol: toluene; n.d.: not detected; c-hex: cyclohexane; cod: 1,5-cyclooctadiene.

Author Manuscript

Author Manuscript

Author Manuscript

Author Manuscript

Author Manuscript

Author Manuscript

Author Manuscript

Author Manuscript

**Table 2.**





Author Manuscript

Author Manuscript

Author Manuscript

Author Manuscript

<sup>a</sup> Conditions: Substrate **3** (0.05 mmol), **2**•[O] (10 mol %), [Ir(*cod*)Cl]<sub>2</sub> (5 mol %), TBABF<sub>4</sub> (10 mol %), PhSiH<sub>3</sub> (3 equiv), 0.05 M in *c*-hex at 45 °C. Isolated yields are given; enantiomeric excess (ee) determined using chiral-phase HPLC.

<sup>b</sup> Column chromatography through NEt<sub>3</sub>-neutralized silica gel was used for purification.

<sup>c</sup> **2**•[O] (25 mol %), [Ir(*cod*)Cl]<sub>2</sub> (12.5 mol %), TBABF<sub>4</sub> (25 mol %), PhSiH<sub>3</sub> (4 equiv), 72 h.